Cross section for stripping of argon ions in atomic collisions with argon gas at energies from 2 to 15 keV per incident charge

S. Bliman, N. Chan-Tung, S. Dousson, B. Jacquot, and D. Van Houtte

S.I.G. and D.R.F./C.P.N. Centre d'Etudes Nucléaires de Grenoble, B.P. 85, 38041 Grenoble, Cedex, France

(Received 30 July 1979)

Cross sections for the stripping of one electron from Ar^+, Ar^{2+}, and Ar^{3+} ions in single collisions on argon atoms have been measured. The measurements were made at energies from 2 to 15 keV per incident-ion charge. The growth-rate method has been used to check that the single-collision condition is realized. Cross sections are then deduced. During the collision, incident ions are scattered out of the acceptance angle of the analyzing device: An estimate of losses is made, and corrected cross sections are proposed. Comparisons to previously published data are attempted: For $\sigma_{1,2}$ one value at 6 keV exists which is in fair agreement with our value; for $\sigma_{2,3}$ our value at 30 keV coincides with the single $\sigma_{2,3}$ value existing.

I. INTRODUCTION

When a beam of atomic ions is passed through matter, electrons may be captured or lost in successive collisions. This causes a distribution of charge states to appear in the ion beam. It is well known that cross sections of large values are associated with electron capture at low energies. Most experimentalists have focused their attention on these phenomena and have neglected stripping. In the range of velocities in excess of 2×10^8 cm/s, stripping cross sections have long been measured since they are useful for calculations of matter stopping power and also for astrophysics and cosmic-ray studies. In the velocity range smaller than 2×10^8 cm/s, which is of great interest in the field of fusion research, there is a lack of measured cross sections. Theoretically calculated cross sections to which data could be compared stem basically from two types of models: the statistical ionization model where agreement with measured values is fair at high energies but poor at low energies for the case of rare-gas ions colliding on the parent gas[1,2]; the two-state theory based on Landau-Zener models[3] is in better agreement with measured values in the energy range close to the $\sigma_{i,i+1}$ maxima. Discrepancies at low energies are important, and they are usually attributed to specific experimental errors such as measurement-device calibration, scattering of projectiles, or the presence of metastable ions in projectile beams.

We report the cross section $\sigma_{i,i+1}$, where i is the incident ion's initial charge state, measurements for the stripping of one electron from Ar ions colliding on Ar targets in the energy range 2–15 keV per incident charge: $\sigma_{1,2}$, $\sigma_{2,3}$, and $\sigma_{3,4}$. The ionization potentials are low compared to the explored energy range. The emphasis has been placed on minimizing sources of errors: elimination of any calibration for measurement devices, since currents associated with the projectile beam and the stripped beam are high enough to be collected on a Faraday cup connected to an electrometer; the angular acceptance of the analyzing magnet is larger than the collision mean scattering angle; it is checked that incident ion beams are free from metastable ions.

II. EXPERIMENTAL DEVICE AND PROCEDURE

Figure 1 is a schematic diagram of the device which has been built. The main elements of the apparatus are as follows. (1) The ion source of the electron cyclotron resonance type,[4] is at positive d.c. high voltage; this potential is variable from 2 to 15 kV. The ion source is pulsed; the square-pulse duration is typically 5 msec, the duty cycle being 0.5. The main characteristics of this source are its low working gas pressure ($\sim 1 \times 10^{-5}$ Torr) and moderate hf power to create the plasma (limited to 500 W). This allows ion-beam formation free from metastables. The extractor is grounded. Typical beam-current values are in the range of 0.1 to 10 μA depending on ion charge and extraction voltage. When extracted, the ion beam is passed through a 167° analyzing electromagnet (2) where a given charge-to-mass ratio is selected.

After this selection, beam shaping is performed with a diaphragm (3), 1 mm in diameter, located before the entrance hole of the gas target. Provision has been made for suppressing secondary electrons on this shaping diaphragm.

A rotatable collector (4) [positioned between diaphragm and collision cell (5)] allows ion-beam-current measurements before entrance in the collision cell. In the absence of target gas, this collector is then used to check total ion-beam transmission through the collision space.
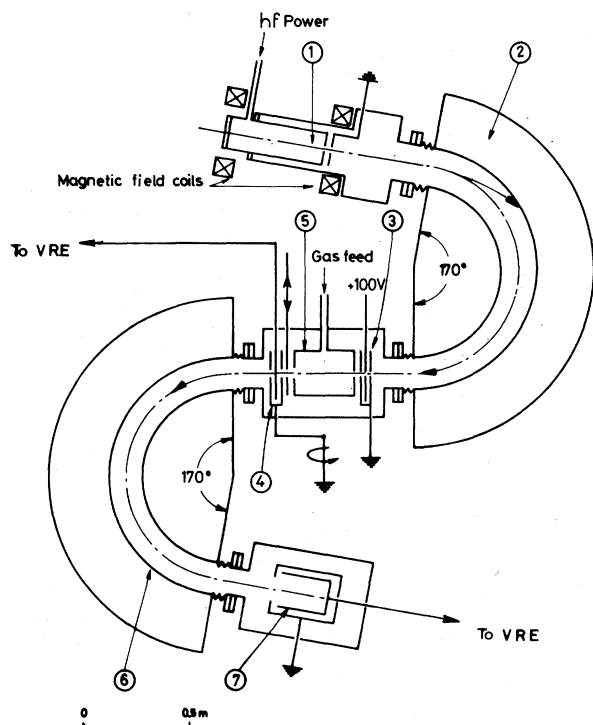

FIG. 1. Schematic diagram of experimental apparatus, where VRE is the vibrating Reed Electrometer: (1)—ion source, (2)—first analyzing magnet, (3)—beam-shaping diaphragm, (4)—rotatable collector, (5)—collision cell, (6) second analyzing magnet, (7)—insulated Faraday cup. Items are described in Sec. II.

A second check of transmission to the Faraday cup (7) is then made by properly adjusting the current to the second analyzing electromagnet (6). Electromagnets (2) and (6) are identical.[5] The ion-trajectory mean radius is constant. Three turbomolecular pumps are used to obtain a base pressure in the device of order 1×10^{-7} Torr, with the ion source in working condition. Gas is fed to the collision chamber, with the pressure varying in the cell from 3×10^{-6} up to 2×10^{-4} Torr. This causes a pressure increase in the surrounding space up to 5×10^{-7} Torr. Pressure measurements in the collision cell and surrounding space are performed using two ionization gauges connected to the same meter.

The collision-chamber entrance hole is 1 mm in diameter. The exit hole is 16 mm in diameter. The length is 182 mm. This defines a conical volume of half angle $\pm 2^\circ 21'$. The angular acceptance of the analyzing magnet is $\pm 3^\circ$ with respect to the incident velocity direction.

At a given setting of the source potential, the charge-to-mass ratio of the beam is magnetically selected. The current incident on collector 4 is measured, then gas is injected into the collision chamber: At every target pressure in the explored range, the current associated with the ion formed during collision is collected on the Faraday cup and measured with the vibrating-reed electrometer. In the high-current limit, the collected currents are measured using a high-gain amplifier (main characteristics; bandwidth 1 MHz, noise limit 10^{-11} A) and the electrometer. This procedure enables comparison of both instruments and extension of the electrometer use to low currents. The form factor is 2 since the square current pulses have a 5 ms duration, with a duty cycle of 0.5.

To analyze the collision products, the magnetic field (6) is swept. As will be seen later, three collisions have been studied:

$$Ar^{+1} + Ar \rightarrow Ar^{2+} + Ar + e^-,$$

$$Ar^{2+} + Ar \rightarrow Ar^{3+} + Ar + e^-,$$

$$Ar^{3+} + Ar \rightarrow Ar^{4+} + Ar + e^-.$$

The stripped product loses both momentum and energy. Identification of the proper charge-to-mass ratio is performed using magnet (6). For a particle of initial charge i and velocity v, the analyzing magnetic field B_i, is associated with the constant radius trajectory $R = mv/eiB_i$.

If its charge changes from i to $i+1$, at constant velocity, the analyzing magnetic field is then lowered, since $R = mv/[e(i+1)B_{i+1}]$. If, furthermore, the ion loses momentum, the analyzing field has to be adjusted at a value slightly smaller than B_{i+1}; this allows momentum-loss measurement $m \Delta v$ and determination of the energy loss.

III. EVALUATION OF DATA—RESULTS

A. Evaluation of data

The growth-rate method has been used to obtain the cross sections associated with the above-mentioned stripping collisions. Neutral gas is injected in the collision cell; at a fixed ion source potential and for each setting of the target pressure, the stripped collision-product current is measured.

If I_b is the incident beam current, the current of stripped ions I_s produced in the path length is given approximately by

$$I_s = I_b N \sigma_{i, i+1},$$

where, N, the target thickness $= 1n$ ($1 =$ target length, $n =$ neutral-gas number density, $\sigma_{i, i+1} =$ collision cross section). In fact, the cross section is associated here to the current collected in the scattering angle accepted by the analyzing magnet.

B. Results

In order to evaluate the cross sections, the basic assumption necessary to use the growth-rate method is that the single-collision condition be satisfied. In other words, the ratio of stripped to incident current has to be a linear function of the target thickness. Figure 2 represents the ratio $I^{2+}/2I^+$ as a function of target pressure, the variable parameter being the source potential. It appears that this ratio has a linear variation over approximately one and one-half orders of magnitude of pressure variation within experimental error. At pressures above $\sim 1 \times 10^{-4}$ Torr, the ratio saturates, showing that the system departs from the single-collision condition. Figure 3 represents the ratio $2I^{3+}/3I^{2+}$ as a function of target pressure, the variable parameter being the source potential. The saturation is seen at pressures in excess of 1×10^{-4} Torr. Figure 4 gives the ratio $3I^{4+}/4I^{3+}$. The linear part extends up to about 1×10^{-4} Torr. This seems to be the limiting value for target pressures to fulfill the single-collision condition. These results have been checked many times, varying essential source conditions to make sure that the cross-section values are not influenced by the presence of ions in metastable states.[6]

In this regard, two source parameters are im-

FIG. 3. Ratio of stripped-ion current to incident-ion current $2I^{3+}/3I^{2+}$ as a function of Ar target pressure. The variable parameter is the source potential $Ar^{2+} \rightarrow Ar^{3+}$.
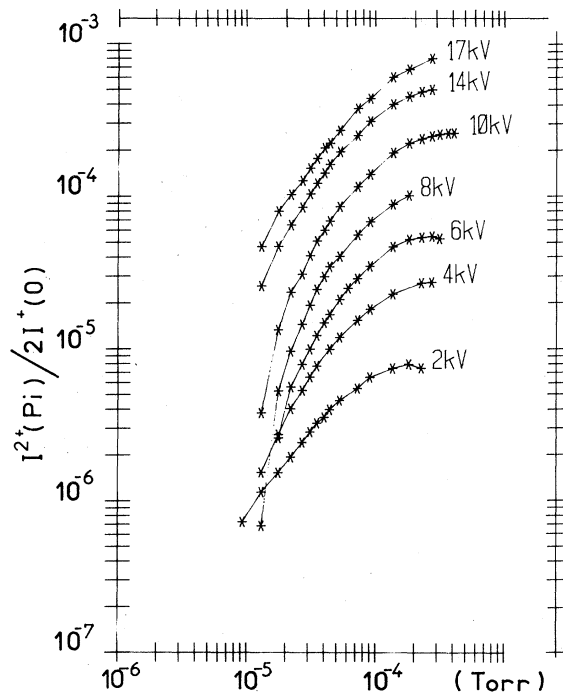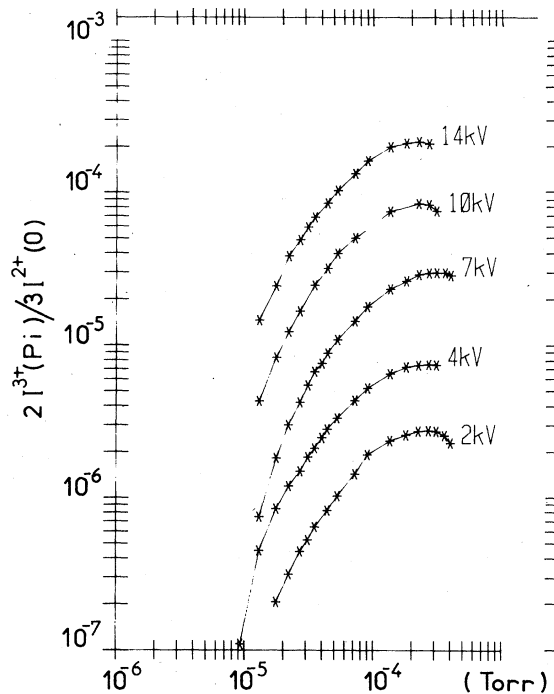
FIG. 2. Ratio of stripped-ion current to incident-ion current $I^{2+}/2I^+$ as a function of Ar target pressure. The variable parameter is the source potential $Ar^+ \rightarrow Ar^{2+}$.
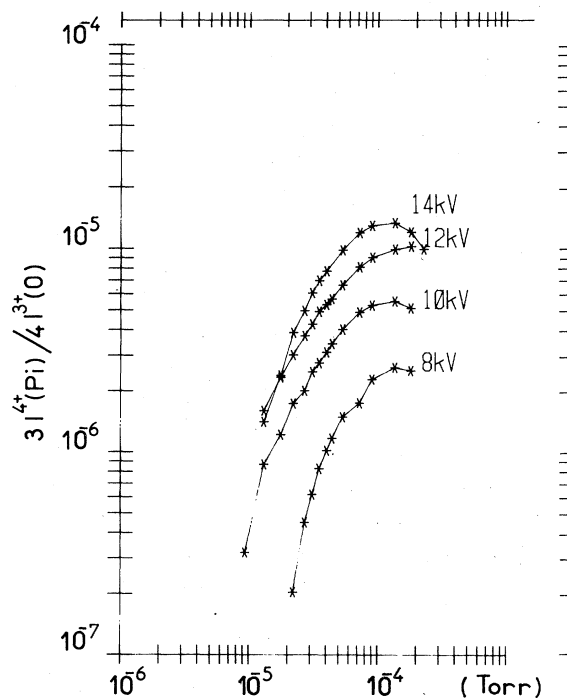
FIG. 4. Ratio of stripped-ion current to incident-ion current $3I^{4+}/4I^{3+}$ as a function Ar target of Ar target pressure. The variable parameter is the source potential $Ar^{3+} \rightarrow Ar^{4+}$.

portant: neutral gasess pressure and hf power level fed to the plasma electrons. Charge-exchange collisions are considered effective in leaving ions in metastable states[6]; in the ion source the charge-exchange collision frequency $n_0 \langle {}_i\sigma_{i-1} v_i \rangle$ – where n_0 is the neutral gas number density, ${}_i\sigma_{i-1}$ the charge-exchange cross section for ion of charge i, v_i the ion velocity in the plasma, which for ion temperatures of 1 eV in the source is of order 10^3 s^{-1}, and $\langle \cdots \rangle$ represents mean value. The probability that ions are left in metastable states in the source is then small. The high-frequency hf power level influences the electron temperature: The excitation rate coefficient is written $\langle \sigma_{exc} v_e \rangle$, and is mostly dependent on σ_{exc}, which is smaller than the ionization cross section by electron impact. Considering the W. Lotz[7] ionization rate coefficients, a collision frequency for ion excitation by electrons can be estimated to be of order 10^3 s^{-1}, a value giving a small probability for collisional excitation. Finally, the ion time of flight from source to target is longer or of the order of the ionic excited-state lifetimes: Typical times of flight are 1×10^{-5} to 5×10^{-6} s for Ar^{3+}, as compared with Ar IV* lifetimes of order 1×10^{-8} to 1×10^{-9} s[8]; for Ar$^+$, 2×10^{-5} to 8×10^{-6} s as compared with Ar II* lifetimes of order 3×10^{-5} to 5×10^{-5} s.[8]

From the stripped current values, correcting for ion losses due to charge exchange in the analyzing magnet,[9] it is possible to obtain the cross section for the stripping of one electron from the projectile, here Ar^{+1}, Ar^{2+}, Ar^{3+}, colliding on Ar as a function of projectile energy. The result is shown on Fig. 5, where $\sigma_{1,2}$, $\sigma_{2,3}$, and $\sigma_{3,4}$ are represented. It is seen that in this energy range, one point for $\sigma_{1,2}$ and one point for $\sigma_{2,3}$ (open square) exist for comparison.

From the measurement procedure an estimate of the relative error in the cross section is made. The relative error is the sum of relative errors on projectile and stripped currents, to which must be added relative errors of pressure and of target length since the stripped ion current is measured in the single-collision condition. The uncertainty on pressure is of order $\pm 10\%$ for the type of ionization gauges used. Owing to entrance and exit holes on the collision chamber, pressure gradients exist at both ends. They may extend over lengths of the order of the hole diameters contributing an additional $\pm 10\%$ error to the interaction length. Adding the errors in the current ($\pm 5\%$), the total error of the measured cross section is then $\pm 25\%$.

In Fig. 5 have also been given values for $\sigma_{1,2}$ at 25, 50, and 100 keV,[10] at 75 keV,[11] and at higher energies[12,13] ($E = 250$–1400 keV), for $\sigma_{2,3}$ and $\sigma_{3,4}$,[14] at 1400 keV. At these high energies, the cross sections seem to reach a maximum. Our results show, at lower energies a steep variation toward a threshold. A net correlation exists between cross sections and ionization potential.

Figure 6 represents relative energy losses for Ar$^+$ undergoing stripping of one electron as function of the incident particle energy. These energy
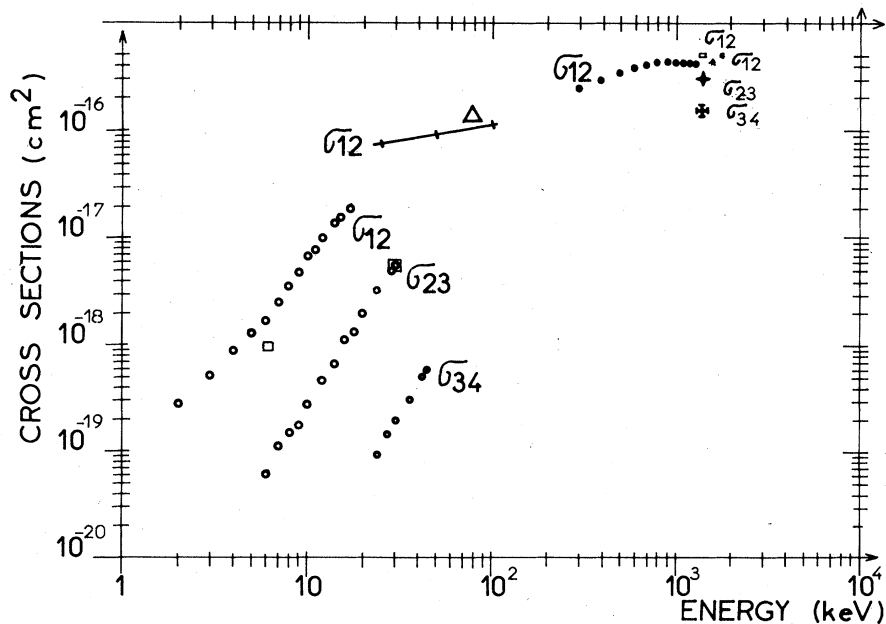

FIG. 5. Stripping cross sections $\sigma_{1,2}$, $\sigma_{2,3}$, $\sigma_{3,4}$ as a function of projectile energy. Present results: open circles; open squares Ref. 6; open triangle Ref. 11; closed circles and + Ref. 12; other symbols Ref. 10.
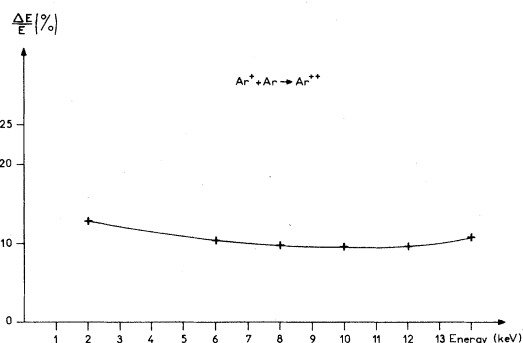
FIG. 6. Relative energy loss of projectile as function of incident-ion energy for $Ar^+ + Ar \rightarrow Ar^{2+}$.

losses are larger than the ionization potential of Ar^+.

IV. DISCUSSION

As has been pointed out by different authors,[10,12,14-16] it is necessary to account for scattering in stripping experiments. From E. Everhart's arguments,[10] considering the geometry of the collision cell and analyzing magnet, an estimate of the current of stripped ions scattered at angles greater than $\pm 3°$ must be made. This angle is the magnet acceptance angle seen from the center of the collision cell. On the average, as the projectile energy decreases, a larger amount of stripped current in a given final charge state is scattered at larger angles.[17] The percentages of total current scattered at angles larger than $4°$ at 25, 50, and

100 keV, as has been measured,[10] are respectively, 28.2%, 12.15%, and 1.3%. This contributes to the total stripping cross section $\sigma_{1,2}$. In the energy range of the present work, percentages of total current for scattering angles greater than $4°$ are estimated, extrapolating from Ref. 10; they are taken as 0.75 at 2 keV, 0.60 at 10 keV, 0.43 at 15 keV, and 0.33 at 20 keV. With these values, an upper limit to the stripping cross section is assigned. This is represented in Fig. 7. From these corrected values, an interpretation is attempted. The Firsov model is considered first for analyzing stripping reactions. In the encounter of colliding atoms, a sort of "frictional heating" of the atomic electron gas takes place leading to the ionization process. The total electron production according to Firsov's theory[1] is given in the form

$$\sigma = \sigma_0 [(v/v_0)^{1/5} - 1]^2 ,$$

with

$$v_0 (cm/s) = [(23 \times 10^6) E_i / (Z_p + Z_t)^{5/3}]$$

and

$$\sigma_0 (cm^2) = [(33 \times 10^{-16}) / (Z_p + Z_t)^{2/3}] ,$$

where v is the projectile velocity, E_i the ionization energy in eV, Z_p and Z_t are the atomic numbers of projectile and target. Introducing mass M and beam energy E, one obtains

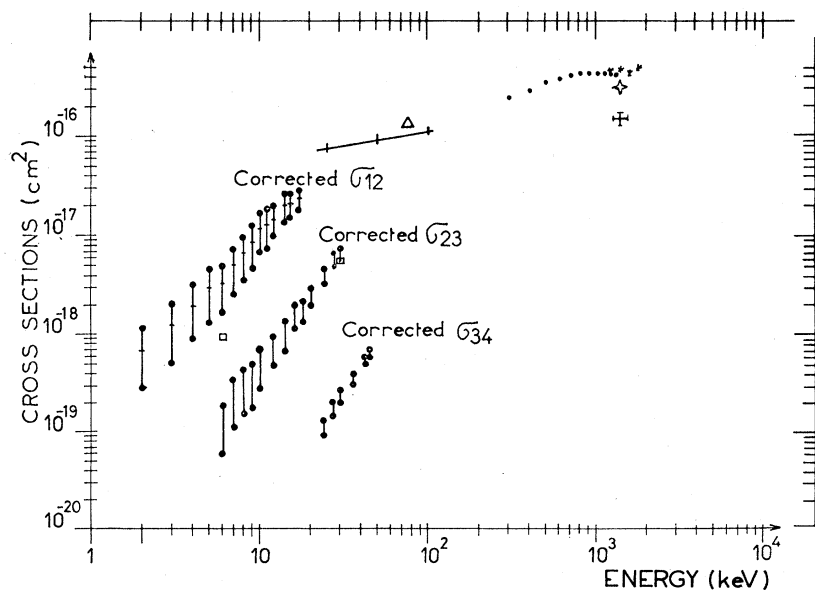$$\sigma/\sigma_0 = [(E/E_0)^{1/10} - 1]^2 ,$$

where

FIG. 7. Stripping cross sections $\sigma_{1,2}$, $\sigma_{2,3}$, $\sigma_{3,4}$ corrected for scattering. The extremity of vertical bars indicates limits on the cross-section values when scattering is estimated.
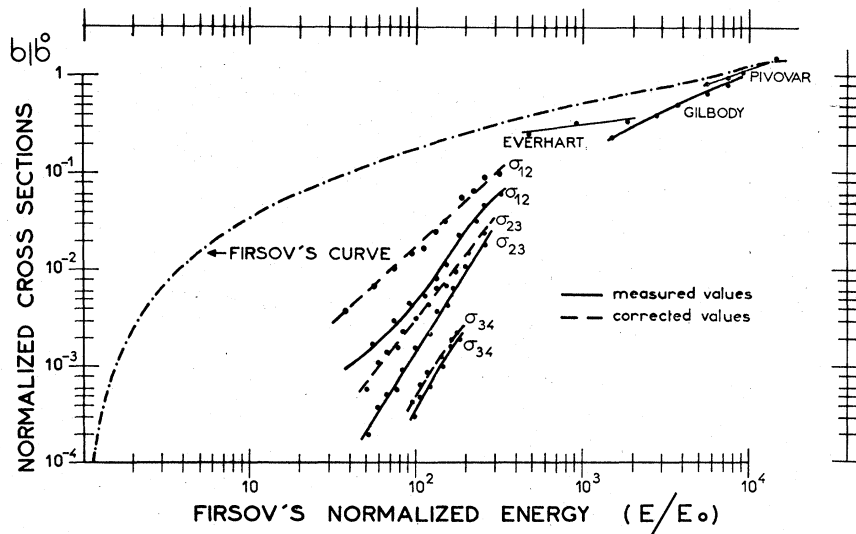
FIG. 8. Comparison of data with Firsov's theory. Normalized cross section as a function of normalized energy (refer to Sec. IV) (dot-dashed line—Firsov's curve; Everhart, Gilbody, Pivovar, refer, respectively, to Refs. 10, 13, and 12).

$$E_0(eV) = 2.7 \times 10^2 M E_i^2/(Z_p + Z_t)^{10/3} .$$

In the relative values σ/σ_0 as a function of E/E_0 Fig. 8 gives the Firsov curve for the Ar : Ar system under consideration (dash-dotted line), points from Refs. 10, 12, and 13, and the present values. At high energies, the agreement is fair. In the low energy limit, this theory is unsatisfactory for comparison. A second approach is made utilizing the two-state model.[3] For practical applications a general expression for the stripping cross section is plotted

$$\delta_{TM}(\epsilon) \approx 3.2 \times 10^{-14}[\epsilon/(\epsilon^{2/3} + 30^{2/3})^3]^{1.2} ,$$

with $\epsilon = E/M E_i^2 R_t^2$. In ϵ, E is the projectile energy, M the atomic mass number of the projectile, E_i the ionization energy of the projectile, and R_t the target radius. In Fig. 9 are represented δ_{TM} (dotted line) and superimposed the present values for $\sigma_{1,2}$. The fit of our $\sigma_{1,2}$ cross-section curve with the two-state model (TM) seems good.

A tentative interpretation of $\sigma_{1,2}$ can be made in terms of molecular orbitals because the probability that an outer-shell projectile electron be
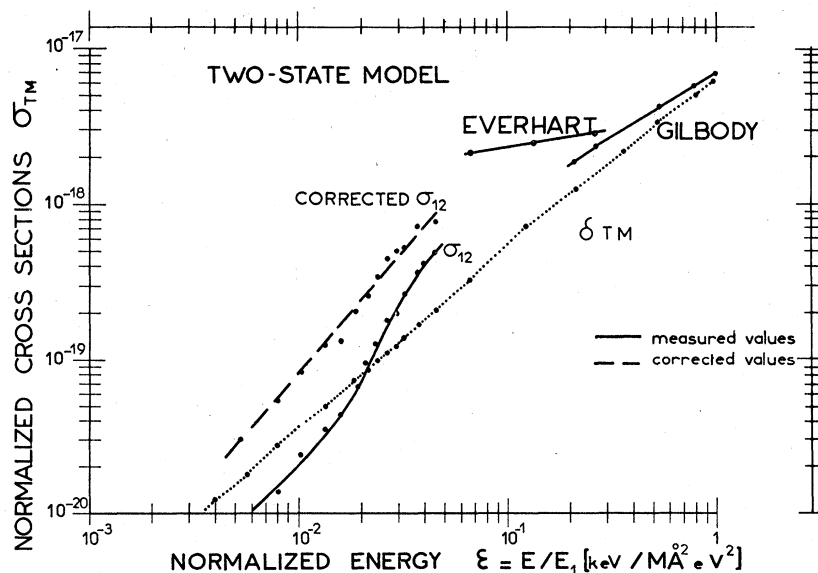

FIG. 9. Comparison of data with the two-state model.[3] The dotted line represents $\delta_{TM}(\epsilon)$ as a function of normalized energy.

POTENTIAL
ENERGY
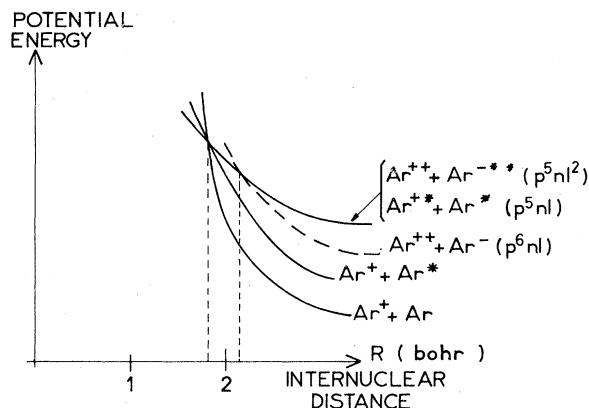

FIG. 10. Schematic representation of potential-energy curves for the system $Ar^+:Ar$.

directly promoted to the continuum is certainly very small.[18] From an inspection of potential-energy curves for the system $Ar^+ - Ar$,[19] it is thought that at close internuclear separation ($R < 2$ bohrs) crossing should take place corresponding to different exit channels, these being schematically represented in Fig. 10. For the situation described in the $\sigma_{1,2}$ measurements, the relevant exit channels could be $Ar^{++} + [Ar^-(p^6nl)]$ breaking to $Ar^+ + e^-$, and $Ar^{++} + Ar^{-**}[p^5nl^2]$ breaking to $Ar^+ + e^- + e^-$. To decide which of them is

dominant requires spectroscopic measurements and an angular analysis of scattered products. From Fig. 6 it is seen that the energy lost by the projectile is larger than the ionization potential. This energy is certainly shared in ionizing one electron plus possibly in exciting target and projectile, with the electron receiving kinetic energy. As to the $\sigma_{2,3}$ and $\sigma_{3,4}$ measurements, there is little work to cite for comparison and discussion. The molecular-orbital approach could certainly be of great help, but no calculations have been performed on $Ar^{2+} + Ar$ and $Ar^{3+} + Ar$ systems.

V. CONCLUSION

Stripping cross sections have been obtained for Ar^{+1}, Ar^{2+}, Ar^{3+} incident on argon targets, in an energy range where until now there were no published data ($E = 2-15$ keV per incident charge). The fit appears to be good for $\sigma_{1,2}$ with a two-state model,[3] but on physical arguments a molecular-orbital analysis[19] would help to clarify some aspects. As for $\sigma_{2,3}$ and $\sigma_{3,4}$, the interpretation is still open.

ACKNOWLEDGMENTS

[1]O. B. Firsov, Zh. Eksp. Teor. Fiz. 36, 1517 (1959) [Sov. Phys.—JETP 9, 1076 (1959)].

[2]A. Russek and M. T. Thomas, Phys. Rev. 109, 2015 (1958).

[3]H. H. Fleischmann, R. C. Dehmel, and S. K. Lee, Phys. Rev. A 5, 1784 (1972).

[4]S. Bliman, S. Dousson, L. Fremion, and R. Geller, Nucl. Instrum. Methods 148, 213 (1978).

[5]P. Griboval, Doctoral thesis, Grenoble, 1966 (unpublished).

[6]A. Müller, M. Klinger, and E. Salzborn, J. Phys. B 9, 291 (1976).

[7]W. Lotz, Z. Phys. 216, 241 (1968).

[8]W. L. Wiese, M. W. Smith, and B. M. Miles, Atomic transition probabilities, Sodium through Calcium (U.S. Dept. of Commerce, Natl. Bur. Stand., Washington, D. C., 1969), Vol. II.

[9]S. Bliman, N. Chan-Tung, S. Dousson, B. Jacquot, and D. Van Houtte (unpublished).

[10]P. R. Jones, F. P. Ziemba, H. A. Moses, and E. Everhart, Phys. Rev. 113, 182 (1959).

[11]D. M. Kaminker and N. V. Ferorenko, Zh. Tekh. Fiz. 25, 1843 1955 [Sov. Phys. Tech. Phys. 1, 1843 (1955)].

[12]L. I. Pivovar, M. T. Novikov, and V. M. Tubaev, Zh. Eksp. Teor. Fiz. 46, 471 (1964) [Sov Phys.-JETP 19, 318 (1964)]; [23, 357 (1966)].

[13]A. R. Lee and H. B. Gilbody, in Proceedings of the Sixth International Conference on Ionization Phenomena in Gases, edited by P. Hubert (S.E.R.M.A., Paris, 1964), Vol. I, p. 123.

[14]I. S. Dimitriev, V. S. Nikolaev, L. N. Fateeva, and Ya. A. Teplova, Zh. Eksp. Teor. Fiz. 42, 16 (1962) [Sov. Phys.—JETP 15, 11 (1962)].

[15]B. Hird and H. C. Suk, Phys Rev A 14, 928 (1976).

[16]C. H. Lane and E. Everhart, Phys. Rev. 120, 2064 (1960).

[17]E. Everhart, G. Stone, and R. J. Carbone, Phys. Rev. 99, 1287 (1955).

[18]M. Barat, J. Baudon, M. Abignoli, and J. C. Houver, J. Phys. B 5, 230 (1970).

[19]V. Sidis, M. Barat, and D. Dhuicq, J. Phys. B 8, 474 (1975).